Available online at www.sciencedirect.com
SCIENCE DIRECT®
Journal of the European Ceramic Society 25 (2005) 3045–3049
www.elsevier.com/locate/jeurceramsoc

Microstructural effects in low loss power ferrites

J. Töpfer [a,*], H. Kahnt [b], P. Nauber [c], S. Senz [d], D. Hesse [d]

[a] *Fachhochschule Jena, FB Werkstofftechnik, Carl-Zeiss-Promenade 2, 07745 Jena, Germany*
[b] *Fachhochschule Jena, FB Elektrotechnik, C.-Zeiss-Promenade 2, 07745 Jena, Germany*
[c] *Tridelta GmbH, M.-Curie-Str. 7, 07629 Hermsdorf, Germany*
[d] *Max-Planck-Institut für Mikrostrukturphysik, Weinberg 2, 06120 Halle, Germany*

Available online 25 March 2005

Abstract

The effect of additions of CaO, SiO_2, SnO_2 and Nb_2O_5 on the microstructure and magnetic properties of Mn–Zn ferrites has been studied. The grain size is determined by the sintering temperature and the concentrations of CaO and SiO_2. TEM studies show that Ca and Si are enriched in thin grain boundary layers and grain junctions. Sn is completely incorporated into the bulk of the ferrite while Nb is found to be segregated at amorphous grain boundary layers. Impedance spectroscopy on CaO- and SiO_2-doped ferrites with fine-grained microstructure reveals an increased grain boundary resistance. The activation energies for charge transport in the bulk and grain boundaries have been verified to be almost identical; thus it is concluded that the microstructure is not formed as a network of isolated grains, but rather by grains which are not completely separated by a very thin insulating film. The power loss is minimum for a homogeneous and fine-grained microstructure which is mainly controlled by CaO and SiO_2 additions and the sintering temperature; Nb_2O_5 and SnO_2 show minor effects.

Keywords: Ferrites; Soft magnets; Grain size; Grain boundaries; Impedance

1. Introduction

Mn–Zn ferrites are important soft magnetic materials for high frequency power electronics. Because of the miniaturization of electronic devices the driving frequency tends to increase to ≥1 MHz. At high frequency the power loss dramatically increases, fostering the development of new low-loss materials. The main contributions to the total loss are hysteresis, eddy current and residual losses, respectively, which predominate at different frequencies.[1] A fine-grained homogeneous microstructure with highly resistive grain boundaries is required to minimize eddy current losses at intermediate and high frequencies.[2,3]

The microstructure of the ferrite is determined by a variety of factors: raw material quality, calcination temperature, milling procedure and sintering regime. Moreover, the concentration of dopants and impurities effectively regulates the densification process and the grain boundary properties. The effect of CaO and SiO_2 on the microstructure and magnetic properties has been studied intensively.[4,5] SnO_2[6] and Nb_2O_5[7] were proposed as additives to be dissolved in the ferrite grains or segregate at grain boundaries, respectively, and decrease losses.

In this contribution we report on Mn–Zn ferrites with additions of CaO, SiO_2 and SnO_2 or Nb_2O_5. The microstructure of the samples is analyzed by TEM and impedance spectroscopy. Correlations between sintering temperature, additive concentration and magnetic properties will be discussed underlining the importance of process control for the preparation of low loss Mn–Zn ferrites.

2. Experimental

Samples of composition 53.1 mol% Fe_2O_3, 11.9 mol% ZnO and 35.0 mol% MnO were prepared by the standard ceramic technology. Raw materials were mixed and calcined at 1050 °C. After addition of 0.02 wt.% SiO_2 and 0.05 wt.% CaO (sample A) or 0.015% SiO_2 and 0.07% CaO (B), or, 0.02% SiO_2 and 0.05% CaO and either 0.1% (C), or 0.2%

* Corresponding author. Tel.: +49 3641 205450; fax: +49 3641 205451.
E-mail address: joerg.toepfer@fh-jena.de (J. Töpfer).

0955-2219/$ – see front matter © 2005 Elsevier Ltd. All rights reserved.
doi:10.1016/j.jeurceramsoc.2005.03.187

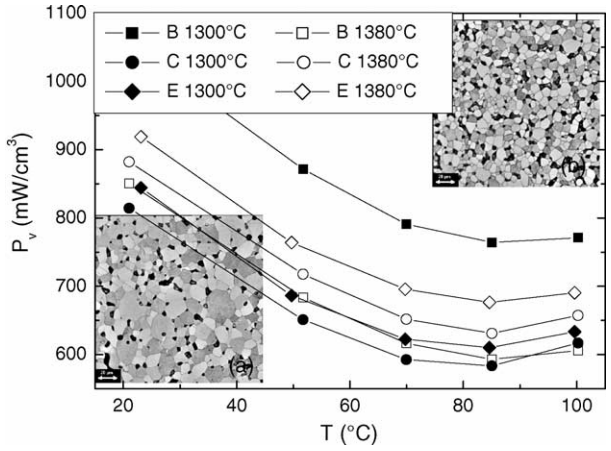

Fig. 1. Power loss at 100 kHz and 200 mT as function of temperature for samples with CaO and SiO_2 addition (B) and with SnO_2 (C) and Nb_2O_5 (E). Inset: SEM micrographs of samples B sintered at 1380 °C (a) and 1300 °C (b).

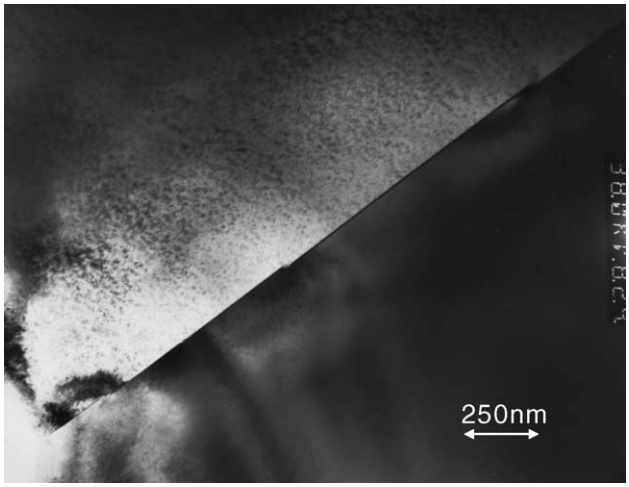

Fig. 2. TEM image of a crystalline grain boundary in sample A (with CaO and SiO_2 additions) sintered at 1380 °C.

(D) SnO_2, or 0.01% (E), or 0.02% (F) Nb_2O_5 the powders were milled in a planetary ball mill to $d_{50} = 4$ μm. After granulation toroids were pressed and sintered at 1300 or 1380 °C and cooled in a O_2/N_2-mixture according to Blank's relation.

The power loss was measured with a power analyzer on toroidal samples. The impedance has been measured with a Solartron FRA1260 between 1 Hz and 32 MHz in the range 140–365 K. The ceramic microstructure was analyzed on polished and chemically etched faces of the magnets by SEM (Zeiss). Transmission electron microscopy (TEM) and energy dispersive analysis of X-rays (EDX) in a scanning TEM (STEM) mode were performed with a Philips CM20FEG microscope.

3. Results and discussion

The physical characteristics and microstructural parameters of samples sintered at 1380 or 1300 °C are summarized in Table 1. The average grain size and density of samples sintered at 1380 °C are larger than those of samples sintered at 1300 °C (Fig. 1). The average grain size is not significantly effected by additions of SnO_2 and Nb_2O_5 (Table 1). On the contrary, the grain size is very sensitive to the concentration of CaO and SiO_2 which has only slightly been varied in this study.

The power loss (Fig. 1) is relatively small for sample B sintered at 1380 °C. Due to the low density of sample B sintered at 1300 °C it appears that P_V (1300 °C) > P_V (1380 °C). For samples C and E, which due to the addition of Sn and Nb show better densification, it follows that P_V (1300 °C) < P_V (1380 °C), which is expected because of the smaller grain size.

Since the additives are expected to form resistive grain boundary phases (CaO, SiO_2, and Nb_2O_5), or to effect the cation distribution in the spinel by incorporation into the ferrite lattice (SnO_2), the additive distribution has been studied by TEM. For sample A (CaO and SiO_2 additions only), amorphous and crystalline grain boundaries were observed. As an example, Fig. 2 shows a crystalline grain boundary with small precipitates which cause small displacements of the grain boundary at the position of the micro-inclusions. In sample D (SnO_2 addition) and F (Nb_2O_5 addition), sintered at 1300 °C, only amorphous grain boundaries or grain junctions were found. A TEM dark field image (Fig. 3) shows a grain boundary with a thickness of about 2 nm starting from a three-grain junction. This grain boundary is amorphous as revealed by incoherent dark field imaging. To detect the distribution of the additive elements in the microstructure, EDX line scans were made through triple junctions of samples D and F. In the SnO_2 doped sample (Fig. 4a) a clear increase of the Ca- and Si-signal in the grain junction is observed, whereas no increased Sn intensity compared to the surround-

Table 1
Density ρ, average grain size d, power loss P_V at 100 kHz, 200 mT, 85 °C and room-temperature conductivity of sintered Mn–Zn ferrites

Sample	T (°C)	ρ (g/cm³)	d (μm)	P_V 85 °C (mW/cm³)	log σ_{tot} 30 °C (Ω cm)$^{-1}$	log σ_g 30 °C (Ω cm)$^{-1}$	log σ_{gb} 30 °C (Ω cm)$^{-1}$
B	1380	4.73	10	593	−2.88	−2.43	−5.92
B	1300	4.43	5.2	764	−3.16	−2.69	−5.93
C	1380	4.81	8.3	630	−2.65	−2.14	−5.54
C	1300	4.60	5.4	583	−2.75	−2.69	−5.93
E	1380	4.78	10.4	616	−2.77	−2.34	−5.81
E	1300	4.56	5.3	610	−2.91	−2.42	−5.70

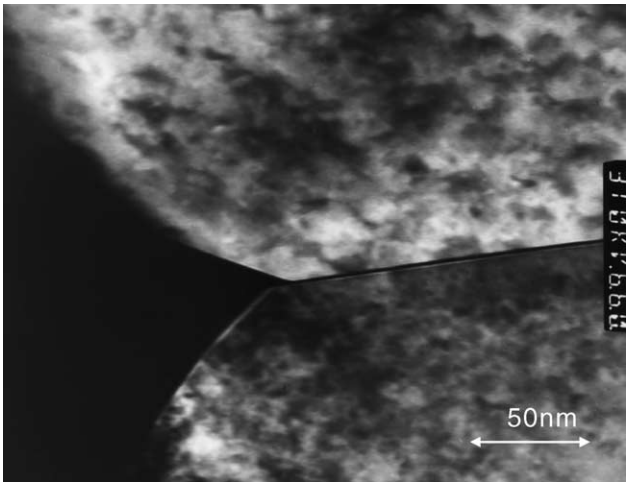

Fig. 3. TEM dark field image of an amorphous grain junction and grain boundary in sample F (with CaO, SiO_2 and Nb_2O_5 additions) sintered at 1300 °C.

ing grains is found. This points to the fact that Sn ions are incorporated into the ferrite spinel lattice, as already reported in ref.[8]. On the other hand, an EDX line scan through a triple junction of a Nb_2O_5 doped ferrite (Fig. 4b) shows enhanced Ca- Si- and Nb-concentrations at the position of the grain junction. This demonstrates, that the majority of the Nb ions form an amorphous boundary phase in combination with Ca and Si. Inaba et al.[7] had reported on the precipitation of crystalline $CaNb_2O_6$ at the grain boundaries and triple junctions; this phenomenon was not observed in this study.

The charge transport behavior of the ferrites and its relation to the microstructure has been studied by impedance spectroscopy. A typical complex plane impedance plot of a sample containing CaO and SiO_2 is shown in Fig. 5. The impedance response has been modeled first by an equivalent circuit of a series arrangement of two parallel *RC*-elements resembling the structural characteristics of the sample, i.e. conductive and capacitive components of grains and grain boundaries connected in series. The impedance is:

$$Z' = \frac{R_g}{1+(\omega R_g C_g)^2} + \frac{R_{gb}}{1+(\omega R_{gb} C_{gb})^2} \quad \text{and}$$

$$Z'' = -\frac{\omega R_g^2 C_g}{1+(\omega R_g C_g)^2} - \frac{\omega R_{gb}^2 C_{gb}}{1+(\omega R_{gb} C_{gb})^2} \tag{1}$$

This equivalent circuit model (model 1) has not proved appropriate to describe the sample's impedance (Fig. 5). Several equivalent circuits with frequency independent *R* and *C* components have been proposed to model the ac-conductivity of ferrites.[9–11] The problem with such an approach is that it does

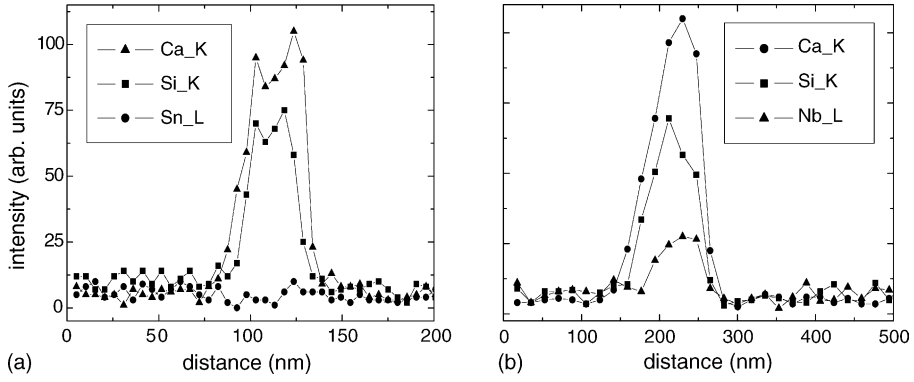

Fig. 4. EDX line scan through a three grain junction of (a) sample D (with CaO, SiO_2 and SnO_2 additions) and (b) sample F (with CaO, SiO_2 and Nb_2O_5 additions).

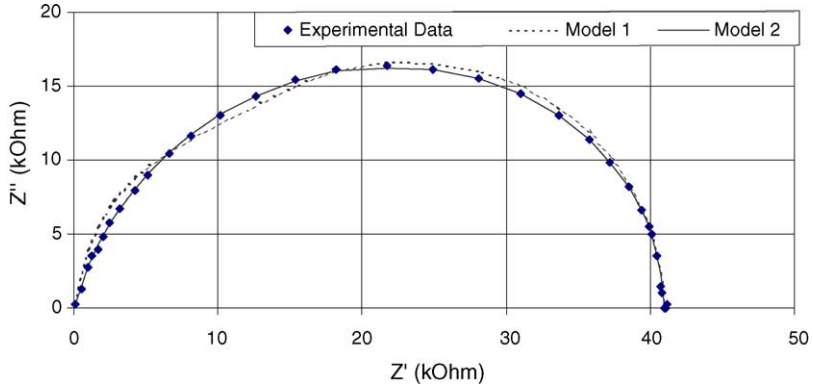

Fig. 5. Complex plane impedance plot at 0 °C of sample B sintered at 1300 °C; fits with serial arrangement of two *RC*-components (model 1) or with two constant phase elements (CPE) (model 2).

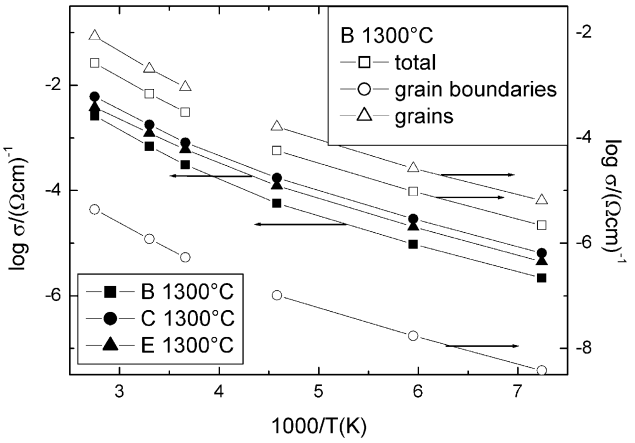

Fig. 6. Temperature dependence of the total dc-conductivity of sample B (addition of CaO, SiO_2); sample C (addition of CaO, SiO_2 and SnO_2) and sample E (addition of CaO, SiO_2 and Nb_2O_5) sintered at 1300 °C and of the grain and grain boundary dc-conductivity of sample B (addition of CaO and SiO_2) sintered at 1300 °C (*y*-axis are shifted for clarity).

not account for the dispersive transport mechanism which is characteristic for hopping-type charge transport between Fe^{2+}/Fe^{3+} sites in ferrites. In this case the typical frequency dispersion of the conductivity can be described according to Davidson and Cole[12] by:

$$\sigma^* = \sigma(0)(1 + i\omega\tau)^n \tag{2}$$

with $\sigma(0)$ is the dc-conductivity, τ the characteristic time constant and $n = 0.6$–0.8.

The total impedance Z^* can be modeled by a series connection of two impedances with frequency dependent components according to Eq. (2) for grain and grain boundary contributions, respectively.

$$Z^* = Z^*_g + Z^*_{gb} = \frac{R_g(0)}{(1 + i\omega\tau_g)^{n_g}} + \frac{R_{gb}(0)}{(1 + i\omega\tau_{gb})^{n_{gb}}} \tag{3}$$

with the grain and grain boundary dc-resistance, $R_g(0)$ and $R_{gb}(0)$, respectively. With $n_g = n_{gb} = 0.8$ this model 2 is shown to fit excellently to the experimental data (Fig. 5).

The ceramic microstructure and the conductivity properties of the microstructural components are reflected in the temperature dependence of the dc-conductivity (Fig. 6). The smaller average grain size of samples sintered at 1300 °C causes a smaller conductivity (Table 1). If due to lowering of the sintering temperature from 1380 to 1300 °C the grain size is reduced, the conductivity decreases by nearly the same factor. Although Nb_2O_5-doped samples have a lower conductivity compared to samples doped with SnO_2 due to the formation of Nb-containing grain boundary phases, a reduction of total conductivity compared to samples doped with CaO and SiO_2 only is not observed. Consequently, a significant reduction of the core loss by Nb- or Sn-doping has not been induced confirming earlier reports on the absence of reduction of losses by SnO_2 addition.[8]

The separation of the total conductivity into contributions from the grains and grain boundaries is obtained from the grain and grain boundary dc-resistance, $R_g(0)$ and $R_{gb}(0)$, respectively. The conductivities are given by

$$\sigma_g = \frac{d}{R_g(0)A}\frac{x}{(1+x)} \quad \text{and} \quad \sigma_{gb} = \frac{d}{R_{gb}(0)A}\frac{1}{(1+x)} \tag{4}$$

with the ratio $x = d_g/d_{gb}$ of the grain diameter and the grain boundary thickness (taken from SEM and TEM images) and d and A as sample dimensions. An example of the temperature dependence of the grain and grain boundary conductivity (Fig. 6) shows that the total conductivity as well as grain and grain boundary conductivity can be divided into a high- and low-temperature range with different activation energies. This might signal a change in the charge transport mechanism. For $T > 0$ °C, the grain- and grain boundary conductivities have identical activation energies (e.g. $E_a = 0.20$ eV for sample B, sintered at 1380 and 1300 °C). This observation is interpreted by assuming that the grains are not completely separated by a non-conducting grain boundary, but have direct contact between some individual ferrite grains which might serve as easy conduction pathways. Such an interpretation of identical E_a for grain and grain boundary transport has been put forward by Macdonald.[13] An experimental confirmation of this hypothesis is shown in Fig. 2, where a close contact of two ferrite grains not separated by an amorphous boundary is documented. The ratio of the conducting pathway area A_{cp} to the total grain boundary area A can be estimated by simple geometrical considerations:

$$\frac{A_{cp}}{A} = \frac{\sigma_{gb}}{\sigma_g} \tag{5}$$

If grain and grain boundary conductivity data are considered with values of the boundary layer thickness in the range of 6–60 nm, the ratio A_{cp}/A is in the order of 10^{-2} to 10^{-3}. This indicates that only a fraction of less than 1% of the contact area between the grains is a conducting pathway.

4. Conclusions

The study of the microstructure and impedance of Mn–Zn ferrites reveals that:

(i) for constant powder morphology the grain size and power loss is mainly determined by the sintering temperature and CaO and SiO_2 additions;
(ii) SnO_2 is dissolved within the spinel grains, whereas Nb_2O_5 is located at grain boundaries and junctions; both additives have minor effects on the power loss;
(iii) the activation energies for charge transport in the bulk and grain boundaries are identical which is interpreted by the appearance of conducting pathways between ferrite grains.

References

1. Stoppels, D., Developments in soft magnetic power ferrites. *J. Magn. Magn. Mater.*, 1996, **160**, 323–328.
2. Takadate, K., Yamamoto, Y., Makino, A., Yamaguchi, T. and Sasada, I., Fine grained Mn–Zn ferrite for high frequency driving. *J. Appl. Phys.*, 1998, **83**, 6861–6863.
3. Jeong, W. H., Han, Y. H. and Song, B. M., Effect of grain size on the residual loss of Mn–Zn ferrites. *J. Appl. Phys.*, 2002, **91**, 7619–7621.
4. Akashi, T., Effect of the addition of CaO and SiO_2 on the magnetic characteristics and microstructures of manganese–zinc Ferrites ($Mn_{0.68}Zn_{0.21}Fe_{2.11}O_{4+\delta}$). *Tran. Japan. Inst. Metals*, 1961, **2**, 171–176.
5. Jeong, G. M., Choi, J. and Kim, S. S., Abnormal grain growth and magnetic loss in Mn–Zn ferrites containing CaO and SiO_2. *IEEE Trans. Magn.*, 2000, **36**, 3405–3407.
6. Minakawa, T., Sato, N. and Nomura, T., Core loss of Mn–Zn ferrite with added SnO_2. *J. Magn. Soc. Jpn.*, 1996, **20**, 497–500.
7. Inaba, H., Abe, T., Kitano, Y. and Shimomura, J., Mechanism of core loss and the grain boundary structure of Nb-doped manganese zinc ferrite. *J. Solid State Chem.*, 1996, **121**, 117–128.
8. Otsuki, E., Yanmada, S., Otsuka, T., Shoji, K. and Sato, T., Microstructure and physical properties of Mn–Zn ferrites for high-frequency power supplies. *J. Appl. Phys.*, 1991, **69**, 5942–5944.
9. Boy, J. H. and Wirtz, G. P., Grain boundary modifications of manganese ferrites. *J. Europ. Ceram. Soc.*, 1994, **14**, 227–235.
10. Nakamura, T. and Okano, Y., Electromagnetic properties of Mn–Zn ferrite sintered ceramics. *J. Appl. Phys.*, 1996, **79**, 7129–7133.
11. Drofenik, M., Znidarsic, A. and Zajc, I., Highly resistive grain boundaries in doped Mn–Zn ferrites for high frequency power supplies. *J. Appl. Phys.*, 1997, **82**, 333–340.
12. Davidson, D. W. and Cole, R. H., Dielectric relaxation in glycerol, propylene glycol and *n*-propanol. *J. Chem. Phys.*, 1951, **19**, 1484–1490.
13. Ross Macdonald, J., *Impedance Spectroscopy*. John Wiley and Sons, New York, 1987, pp. 191–197.